Distinct roles of PTCH2 splice variants in Hedgehog signalling

Fahimeh RAHNAMA, Rune TOFTGÅRD[1] and Peter G. ZAPHIROPOULOS[1]

Department of Biosciences at Novum, Karolinska Institute, Huddinge 141 57, Sweden

The human *PTCH2* gene is highly similar to *PTCH1*, a tumour suppressor gene frequently mutated in basal cell carcinoma and several other tumour types. PTCH1 is a transmembrane protein believed to inhibit another transmembrane protein SMO (Smoothened), which mediates HH (Hedgehog) signalling. In this study, we analysed the biological properties of several PTCH2 splice variants. An mRNA form that lacked the last exon was abundantly expressed in all tissues examined, in contrast with the one that included it. Moreover, a transcript lacking exon 9, which is a part of a conserved sterol-sensing domain, was identified in intestine, prostate and cerebellum. In ovary, spleen, testis, cerebellum and skin, an mRNA lacking both exons 9 and 10 could also be observed. The different PTCH2 isoforms localized in the cytoplasm were capable of internalizing the N-terminal fragment of Sonic HH (Shh-N). Additionally, the *PTCH2* gene was found to be a target of HH signalling. *PTCH2* promoter regulation assays demonstrated that only one of the PTCH2 variants could inhibit the activity of SHH-N, whereas none was capable of inhibiting the activated form of SMO (SMO-M2) and this contrasts with PTCH1. Despite the fact that the PTCH2 isoforms lacked the ability to inhibit SMO-M2 activity, all PTCH2 variants as well as PTCH1, on co-transfection with Smo, were able to change Smo localization from being largely dispersed in the cytoplasm to the juxtanuclear region. Furthermore, the PTCH2 isoforms and PTCH1 co-localized in doubly transfected cells and an interaction between them was confirmed using immunoprecipitation assays. Using *Ptch1*$^{-/-}$ mouse cells, it was shown that the PTCH2 variants and PTCH1 differentially act to reconstitute not only the SHH- but also the Desert HH-dependent transcriptional response. We conclude that in spite of their structural similarities, the PTCH2 isoforms have distinct functional properties when compared with PTCH1.

Key words: DHH (Desert Hedgehog), *PTCH1* tumour suppressor gene, PTCH2, SHH (Sonic Hedgehog).

INTRODUCTION

PTCH1 is a tumour suppressor gene underlying the nevoid BCC (basal cell carcinoma) syndrome, an autosomal dominant disorder characterized by multiple developmental abnormalities and predisposition to BCC and other tumours [1,2]. In the non-signalling state, PTCH1 is thought to inhibit the constitutive signalling of another membrane protein SMO (Smoothened). Binding of SHH (Sonic Hedgehog) to PTCH1 releases this inhibition allowing signalling to be transduced to a microtubule-associated complex. This complex is best characterized in *Drosophila* and contains a number of intracellular components including costal2, a protein with kinesin-like motif, the serine/threonine kinase fused, suppressor-of-fused and the zinc-finger-containing transcription factor *Cubitus interuptus* (ci). Furthermore, dispatched and tout-velu are two proteins involved in modulating hh (Hedgehog) signalling in secreting and receiving cells respectively [3,4].

The hh family includes secreted proteins that undergo autocatalytic cleavage and modification to give a 20 kDa, active N-terminal fragment covalently bound to cholesterol [5] and palmitic acid [6]. Mammals have three different types of HH proteins, SHH, Indian HH and DHH (Desert HH), two patched receptors, PTCH1 and PTCH2 and three ci-like proteins, GLI1, GLI2 and GLI3 [7]. In addition, mammals have a HH-interacting protein, not found in *Drosophila*, which appears to function as a regulator of ligand availability [8]. Moreover, different isoforms of several key components in this pathway have been observed in mammals. For example, expression of alternative first exons of the human *PTCH1* gene is differentially regulated in normal tissues and tumours, with the alternative first exon, exon 1B, being required for full inhibition of SMO signalling [9]. On the other hand, deletion of the last 156 amino acids of *Drosophila* ptch ectopically activates the hh pathway, suggesting that these amino acids are required to repress signalling in the fly [10]. Finally, expression of three different 5′-untranslated regions in GLI1 mRNAs transcripts has been observed in mouse and human tissues. Post-transcriptional regulation of GLI1 appears to be mediated by exon skipping of these untranslated exons and an association of the most efficiently translated GLI1 mRNA with BCC has been observed [11].

The second to sixth transmembrane domains of PTCH1 show high similarity to the cholesterol-sensing motif of the Niemann–Pick disease protein and 3-hydroxy-3-methylglutaryl-CoA reductase [12,13]. The function of this similar domain is not known and so far there is no evidence that PTCH1 participates in cholesterol homoeostasis, but this motif may have a role in modulating signalling. *Drosophila* ptch with mutations in this SSD (sterol-sensing domain) acts in a dominant-negative pattern, causing derepression of hh target genes. This is in spite of the fact that the mutants are able to bind hh [14,15]. However, similar mutations in this region in mouse Ptch1 did not yield comparable results, highlighting functional differences between vertebrates and flies [16].

PTCH2, a gene similar to *PTCH1*, was identified in our laboratory and localized to the short arm of chromosome 1(1p32.1–32.3) [17]. *PTCH2* comprises 23 coding exons and spans approx. 15 kb of genomic DNA. The gene encodes a 1203 amino acid

Abbreviations used: BCC, basal cell carcinoma; HA, haemagglutinin; HH, Hedgehog; DHH, Desert HH; SHH, Sonic HH; HEK-293, human embryonic kidney 293 cells; SMO, Smoothened; SSD, sterol-sensing domain.

[1] Correspondence may be addressed to either author (e-mail rune.toftgard@cnt.ki.se or peter.zaphiropoulos@cnt.ki.se).

Table 1 Sequence of the primers used for tissues distribution analysis

Primer name	Primer sequence
(8)–(11) forward	5′-GGAGGCATGGCCAGAG
(8)–(11) forward nested	5′-GTGCTACAAGCCTGGCA
(8)–(11) reverse	5′-AAGCCCAGTCCTGGTCA
(8)–(11) reverse nested	5′-CCGATTCCCAGAGCCAA
(19)–(int21)(22) forward	5′-TGGCGTTGAGTTCACAGT
(19)–(int21)(22) forward nested	5′-GCTTGCTGGTTCCCACT
(19)–(int21) reverse	5′-GGTCTCTGTGCTTCAGC
(19)–(int21) reverse nested	5′-CCAGAGCTAGTGGCAGCA
(19)–(22) reverse	5′-TCAGCCTGTCCAGACAG
(19)–(22) reverse nested	5′-GGAGGCAGAGGCTAGAT

putative transmembrane protein. PTCH2 is 57 % identical with PTCH1. It diverges from PTCH1 mostly in the hydrophilic region between transmembrane domains 6 and 7. Additionally, PTCH2 lacks the C-terminal extension present in mouse, chicken and human PTCH1 [18,19].

The physiological function of PTCH2 is still unknown. Most experiments have been focused on PTCH1 but it is known that *Ptch1* and *Ptch2* are differentially expressed in mouse during epidermal development [20]. Tissue distribution analysis indicates that PTCH2 is preferentially expressed in skin and testis. Binding analysis shows that both PTCH1 and PTCH2 can interact with all HH family members with similar affinity and form a complex with SMO [21]. Suppression of hair follicle development inhibits induction of *Shh*, *Ptch1* and *Ptch2* in hair germs in mice [22]. Thus PTCH2 appears to be involved in SHH/PTCH cell signalling. However, PTCH2 mutations are very rare events in medulloblastomas and BCCs [23]. Moreover, the fact that the mutated PTCH1 in BCCs cannot be replaced by overexpressed PTCH2 implies that PTCH2 has related, but yet distinct functions when compared with PTCH1 [17].

In this study, we analysed the functional properties of three PTCH2 splice variants in relation to PTCH1 within the context of the HH signalling pathway. Differences in the ability to modulate signalling were revealed among these isoforms of PTCH2. However, PTCH1 was consistently characterized by a stronger inhibitory activity when compared with any of the PTCH2 variants.

MATERIALS AND METHODS

Tissue distribution analysis

The multiple tissue cDNA (MTC™) panel from ClonTech Laboratories (Palo Alto, CA, U.S.A.), cerebellum cDNA (ClonTech Laboratories) and skin cDNA, as described before [9], were used to detect PTCH2 splice variants by PCR. The primers were obtained from Cybergene AB (Huddinge, Sweden) (Table 1). Each reaction consisted of 5 μl of 10× buffer B (Promega, Madison, WI, U.S.A.), 8 μl of dNTP mixture (1.25 mM each), the required amount of each primer to reach 0.5–1.0 mM, 1.0 μl of *Taq* DNA polymerase (5 units/μl), 4 μl of $MgCl_2$ (25 mM) and 5 μl of cDNA in a total volume of 50 μl. Thirty cycles with 1 min at 95 °C, 1 min at 54 °C and 1 min at 72 °C were performed on a PerkinElmer thermocycler. For nested PCR, 0.5 μl of the initial amplification products was used. Amplifications without exogenous cDNA were used in all sets of experiments as a negative control. The nested products were analysed on a 4 % NuSieve 3:1 agarose gel (FMC BioProducts, Rockland, ME, U.S.A.). All PCR products were cloned and sequence-verified (Cybergene AB).

Expression constructs

Overlap PCR was used to generate constructs for the full-length cDNA of PTCH2 and the observed splice variants. Different clones obtained by 5′-RACE (rapid amplification of cDNA ends)–PCR in combination with the 3′-end of the Incyte PTCH2 clones [17] were therefore used with the Advantage HF™ PCR kit (ClonTech Laboratories). Three constructs were made. The full-length PTCH2 that included exons 20, 21 and 22 (PTCH2), PTCH2-Δ22 that has the last exon substituted by 'intronic' sequence and PTCH2-Δ9,10 that lacks exons 9 and 10. We chose to use the 3′-end region present in PTCH2-Δ22 for this last construct because of the detection of that 3′-end transcript in all tissues examined. The amplified cDNAs for each construct were inserted into the pcDNA3.1/His B (Invitrogen, Carlsbad, CA, U.S.A.) mammalian expression vector. The primer sequences used for overlap PCR are available on request.

A full-length 3′-FLAG tagged PTCH1 construct with the alternative first exon, exon 1B [9], was used. The insert was also subcloned into pcDNA3.1/His A (Invitrogen) to generate PTCH1/PTCH2 expression constructs with the same vector backbone.

A cDNA construct containing the human N-terminal DHH cDNA was generated from testis RNA as follows: a mixture of 4 μl of $MgCl_2$ (25 mM), 2 μl of reverse transcription 10× buffer (Promega), 2 μl of dNTP mixture (10 mM), 0.5 μl of recombinant RNasin® RNase inhibitor, 0.75 μl of avian myeloblastosis virus reverse transcriptase (15 units), 1 μl of DHH-specific primer (5′-AGGCGCACAGTTGCA) (0.5 μg) and 10 μg of total RNA was incubated for 60 min at 42 °C. The single-stranded cDNA was subsequently used for PCR to amplify a region of approx. 600 bp in DHH, which corresponds to that of the SHH expression construct (see below). The forward primer 5′-GCGGTACCATGGCTCTCCTGACCAATC and the reverse primer 5′-GCGAAGCTTTTTCCCGGAAAGCAGCCG were flanked by *Kpn*I and *Hin*dIII sequences. The PCR fragment was cloned into *Kpn*I–*Hin*dIII-digested CMV5 vector. All constructs were verified by sequencing (Cybergene AB).

Other expression constructs used were the human N-terminal SHH, the HA (haemagglutinin)-tagged Smo and the human full-length GLI1 which have been described before [24], and the activated human SMO-M2 [25].

RNase protection assay

A construct containing exon 8 spliced to exon 11 and an additional one with exon 20 spliced to exon 21 flanked by 'intronic' sequence were generated by PCR amplification (25 cycles) with the Advantage HF™ PCR kit (ClonTech Laboratories) using the PTCH2-Δ9,10 expression construct as template. The primers were the previously used (8)–(11) forward nested, (8)–(11) reverse nested and (19)–(int21) reverse nested and a novel exon 20 forward primer (5′-TGACAGTGCTCACGCTC). PCR products were cloned into the pGEM-T vector (Promega) and the identity of the constructs was verified by sequencing (Cybergene AB). The exon 8–11 construct was linearized with *Sph*I and *Nco*I (Promega), whereas the exon 20–21 construct was linearized with *Not*I and *Sal*I (Promega). cRNAs were transcribed (MAXIscript™; Ambion, Austin, TX, U.S.A.) in the presence of ^{32}P-labelled UTP (Amersham Biosciences, Little Chalfont, Bucks., U.K.) with either SP6 polymerase (exon 8–11) or T7 polymerase (exon 20–21). Total RNA (20 μg) from human testis (ClonTech Laboratories) was incubated with equal amounts of the two riboprobes and subjected to RNase protection analysis following the method of the RPA III™ kit (Ambion). Electrophoretic separation of the riboprobes and the protected fragments were performed on

denaturing 8 and 10 % acrylamide/urea gels and visualized after exposure to Fuji Super RX film.

Immunofluorescence

Cells transfected with PTCH2 variants, PTCH1 and Smo expression constructs or incubated with Shh-N were permeabilized and blocked in PBS + 0.5 % Triton X-100 + 10 % normal donkey or rabbit serum for 1 h at room temperature (22 °C). Subsequently, cells were incubated in primary antibodies followed by secondary antibodies diluted in blocking solution for 1 h at room temperature. Washes were performed twice with PBS between each incubation. The following antibodies were used: Patched2 (M-20) (Santa Cruz Biotechnology, Santa Cruz, CA, U.S.A.) at 1:400 dilution; anti-Xpress™ mAb (monoclonal antibody; Invitrogen) at 1:100 dilution; Shh (N-19) goat antibody (Santa Cruz Biotechnology) at 1:50; rabbit PTCH-C antibody against the C-terminal 18 amino acids [9] at 1:200; HA antibody (Santa Cruz Biotechnology) at 1:400; Fluorescein-conjugated donkey anti-goat IgG (Jackson Immunoresearch Laboratories, West Grove, PA, U.S.A.) at 1:400; Rhodamine Red™-X-conjugated donkey anti-mouse IgG (Jackson Immunoresearch Laboratories) at 1:400; fluorescein-conjugated donkey anti-rabbit IgG (Jackson Immunoresearch Laboratories) at 1:400 or fluorescein-conjugated rabbit anti-goat IgG (Jackson Immunoresearch Laboratories) at 1:400 dilution.

For nuclear staining (see Figure 4b), cells were incubated with 5 μM DRAQ™ (Alexis Biochemical, Montreal, Canada) in PBS for 10 min, after incubation with fluorescein antibody.

Immunoprecipitation and Western blotting of PTCH1, PTCH2 and DHH

PTCH1 and/or PTCH2-transfected HEK-293 (human embryonic kidney 293) cells were lysed in PBS buffer, supplemented with 1 % Nonidet P40, protease inhibitors and 0.5 % deoxycholic acid. Immunoprecipitation was performed with anti-Xpress™ mAb (Invitrogen) or FLAG m2Ab (Stratagene) followed by Protein G plus Protein A–agarose beads and then separated on 6 % SDS/polyacrylamide gel. Proteins were transferred on to a PVDF membrane (Millipore, Billerica, MA, U.S.A.) and probed with a 1:1000 dilution of anti-Xpress™ mAb (Invitrogen) or a 1:2000 dilution of FLAG m2Ab (Stratagene) following blocking in 10 % fat-free milk in PBS. As a secondary antibody, a conjugated horseradish peroxidase antimouse Ig was used at a 1:2000 dilution. ECL® (enhanced chemiluminescence) detection (Pierce) was performed according to the manufacturer's instructions. To calculate the percentage of PTCH1 that is retained in the immunoprecipitate, the observed signal intensities in the cell lysate and immunoprecipitation complex were adjusted for an equivalent amount of starting material.

For DHH detection, HEK-293 cells were transfected with the DHH expression construct. Cells were lysed and processed as above. As primary antibody, a Dhh (N-19) goat antibody (Santa Cruz Biotechnology) at 1:200 dilution, and as secondary antibody, a conjugated horseradish peroxidase antigoat Ig at 1:2000 dilution, were used.

SHH internalization assay

C3H/10T1/2 cells were transfected with PTCH1 or PTCH2 anti-Xpress constructs. Cells were incubated 48 h after transfection, at 37 °C for 2 h with 1 nM Shh-N peptide (R&D Systems, Minneapolis, MN, U.S.A.). Cells were washed, fixed and processed for detection of PTCH1, PTCH2 and Shh-N immunofluorescence.

PTCH2 reporter gene construct

A BAC clone harbouring the *PTCH2* gene was obtained from Genome System™ by custom library screening using PTCH2 primers (available on request). By primer walking, approx. 4 kb of the genomic region upstream of exon 1 was sequenced (Cybergene AB). A fragment of approx. 3.4 kb of the 5′-regulatory region, including the ATG codon in exon 1, was amplified using the Advantage HF™ PCR kit (ClonTech Laboratories) and subcloned into pGL3-Basic vector (Promega). This sequence corresponds to nucleotide positions 18333–21786 in the recently deposited GenBank entry (accession no. GI: 19031310), which contains the complete *PTCH2* gene. This construct (*PTCH2*-luc) was verified by sequencing (Cybergene AB).

Transfection assays

Confluent cultures of NIH-3T3 cells were trypsinized and plated at 1:6 dilution on 24-well plates. The next day, cells were transfected with 0.2 μg of β-galactosidase control (RSV-lacZ), 0.2 μg of PTCH2-luc reporter and 0.2 μg of expression constructs, unless indicated otherwise, using 3 μl of Fugene (Roche) transfection reagent. pcDNA3.1/His B (Invitrogen) was used to reach a concentration of 1.6 μg of total DNA/well. After the cells had reached saturation density (1–2 days), the medium was changed to 0.5 % bovine calf serum and the cells were lysed 24 h later. Luciferase activity was measured using the Luciferase Assay kit (BioThema, Haninge, Sweden). Galactosidase activity was measured using Galacto-Light kit (Applied Biosystems, Foster City, CA, U.S.A.).

Confluent *Ptch1*$^{-/-}$ cells were plated at 1:8 dilution on 24-well plates. The next day, cells were transfected with 0.2 μg of PTCH2-luc reporter, 0.2 μg of SHH-N or 0.2 μg of DHH-N and 1 μg of PTCH1/PTCH2 expression constructs, unless indicated otherwise, and 50 ng of *Renilla* luciferase (pRL-SV40) as transfection control. Fugene (3 μl; Roche) was used with an equal amount of DNA/well (1.45 μg) reached by using pcDNA3.1/His B (Invitrogen). Normalized luciferase activity was determined with the dual-luciferase reporter assay system (Promega) using the Microplate Luminometer (Berthold Detection System, Pforzheim, Germany).

All experiments were repeated independently at least three times and measurements in each experiment were performed at least twice.

RESULTS

Expression analysis of PTCH2 splice variants in normal tissues

The original studies, describing the isolation of the PTCH2 cDNA, reported the presence of several splice variants [17]. Two of these are probably of significant biological importance: (a) a variant in the 3′-end region that changes the last four coding amino acids to 61 novel ones originating from the terminal 'intron', PTCH2-Δ22 (Figure 1) and (b) a variant that skips exons 9 and 10, with the open reading frame being maintained at the exon 8 to 11 junction, PTCH2-Δ9,10 (Figure 2). This region encodes the last segment of the first extracellular loop in the putative structure of PTCH1 and overlaps with the SSD motif [26], whereas the C-terminal region is thought to have a role in repressing signalling [10]. Consequently, we initially wanted to examine the expression pattern of these variants.

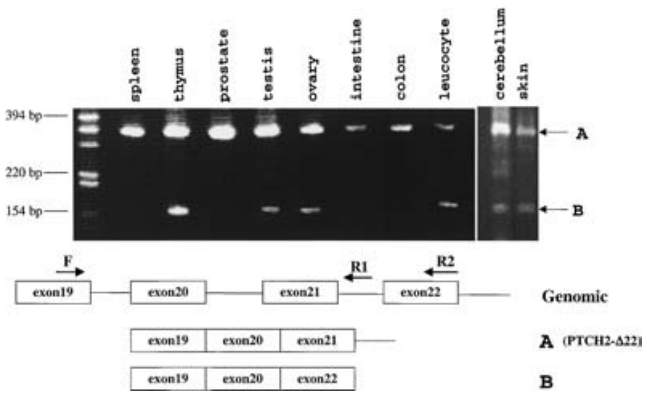

Figure 1 Expression analysis of the 3′-end of PTCH2 in different tissues

Agarose gel electrophoresis of the PCR products obtained by amplifying cDNA from various tissues using exon 19 forward primers combined with both exon 22 and 'intron 21' reverse primers (see the Materials and methods section). The individual tissues are indicated on top and the molecular-mass markers to the left. The structure of the genomic DNA (not drawn to scale) and the detected transcripts are indicated by A and B.

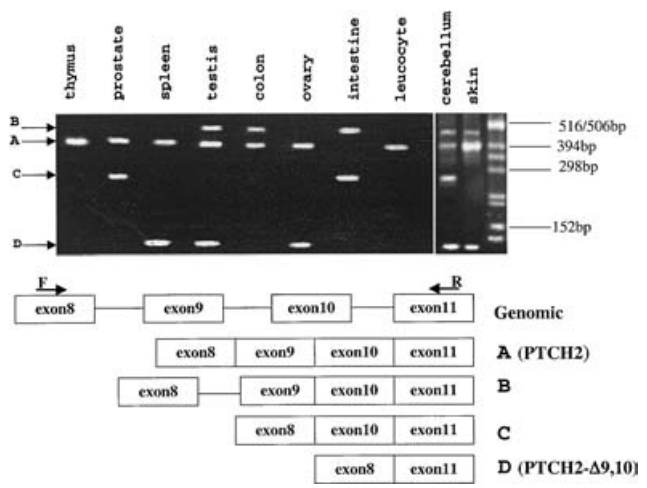

Figure 2 Expression analysis of the exons 8–11 segment of PTCH2 in different tissues

Agarose gel electrophoresis of the PCR products obtained by amplifying cDNA from various tissues using exon 8 forward primers combined with exon 11 reverse primer (see the Materials and methods section). The individual tissues are indicated on top and the molecular-mass markers to the right. The structure of the genomic DNA (not drawn to scale) and the detected transcripts are indicated by A–D.

Using a cDNA panel (ClonTech Laboratories) as well as cerebellum (ClonTech Laboratories) and skin cDNA [9], the region between exon 19 and the last exon, exon 22, of the PTCH2 transcripts was specifically amplified. The splice variant that had the last exon substituted by 'intronic' sequences, PTCH2-Δ22, was abundantly expressed in all tissues examined. Strikingly, the full-length PTCH2 that includes exons 19, 20, 21 and 22 could not be observed in any tissue. However, a transcript lacking exon 21, with exon 20 joined to exon 22, could be observed in thymus, testis, ovary, leucocytes, cerebellum and skin (Figure 1). Most interestingly, this exon 20 to 22 splicing event changes the reading frame of exon 22, resulting in the introduction of 26 novel C-terminal residues. The relative level of expression of this exon 21-skipped transcript was lower than that of PTCH2-Δ22.

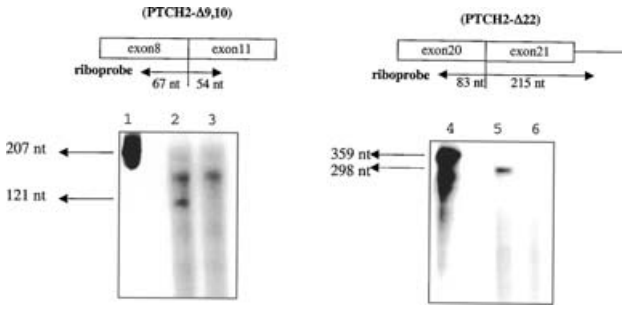

Figure 3 RNase protection assay for PTCH2-Δ9,10 and PTCH2-Δ22 transcripts

Analysis of PTCH2 splicing variants by the RNase protection assay. Lane 1, undigested riboprobe-containing exons 8–11; lane 2, exons 8–11 riboprobe incubated with 20 μg of total RNA from human testis and subjected to RNase digestion; lane 3, exons 8–11 riboprobe subjected to RNase digestion without added human testis RNA; lane 4, undigested riboprobe containing exons 20–21; lane 5, exons 20–21 riboprobe incubated with 20 μg of total RNA from human testis and subjected to RNase digestion; lane 6, exons 20–21 riboprobe subjected to RNase digestion without added human testis RNA.

The same methodology was also used to analyse the expression pattern of the region between exons 8 and 11 in the same cDNAs (Figure 2). The transcript that had these four exons spliced together, PTCH2, was present in all tissues except intestine. This tissue as well as testis, colon, cerebellum and skin contained cDNAs that had not excised intron 8, resulting in a shift of the reading frame and premature termination. Moreover, a transcript that lacked exon 9 was found in prostate, intestine and cerebellum. This skipping event, however, maintained the reading frame at the exon 8 to 10 junction. Additionally, the transcript that lacked both exons 9 and 10, PTCH2-Δ9,10, was observed in spleen, ovary, testis, cerebellum and skin.

To obtain additional evidence by a non-PCR-based method for the presence of mRNAs encoding PTCH2-Δ9,10 and PTCH2-Δ22, RNase protection analysis was employed using human testis as the RNA source. Two riboprobes were generated with sizes of 207 bases for exons 8–11 and 359 bases for exons 20–21. As anticipated, protected fragments with sizes of 121 bases for exons 8–11 and 298 bases for exons 20–21 were clearly visible (Figure 3), confirming the results from the PCR analysis.

PTCH2 variants code for proteins that localize in the cytoplasm

Since detection of endogenous PTCH2 in various cell lines by Western-blot analysis was not possible, we generated expression constructs for three of these variants, the full-length PTCH2, PTCH2-Δ22 and PTCH2-Δ9,10. A similar construct for PTCH1 was also generated as control. These constructs contained an anti-Xpress epitope tag at their N-terminus and were transiently transfected into COS7 cells. Additionally, the expression of endogenous PTCH2 in NIH-3T3 cells transfected with GLI1 was analysed. The localization of the corresponding proteins was determined either by indirect immunofluorescence using an antibody against the epitope tag or directly against PTCH2. The three PTCH2 variants, PTCH1 and the GLI1-induced endogenous PTCH2 localized mostly in cytoplasmic structures that may represent intracellular vesicles as has also been reported for PTCH1 [27] (Figure 4), with no major differences among them. To verify the specificity of the antibody detecting endogenous PTCH2, epitope-tagged PTCH2-Δ22 construct was used to transfect COS7 cells. Expressing cells were clearly detected using the antibody against PTCH2 (Figure 4b), and similar results

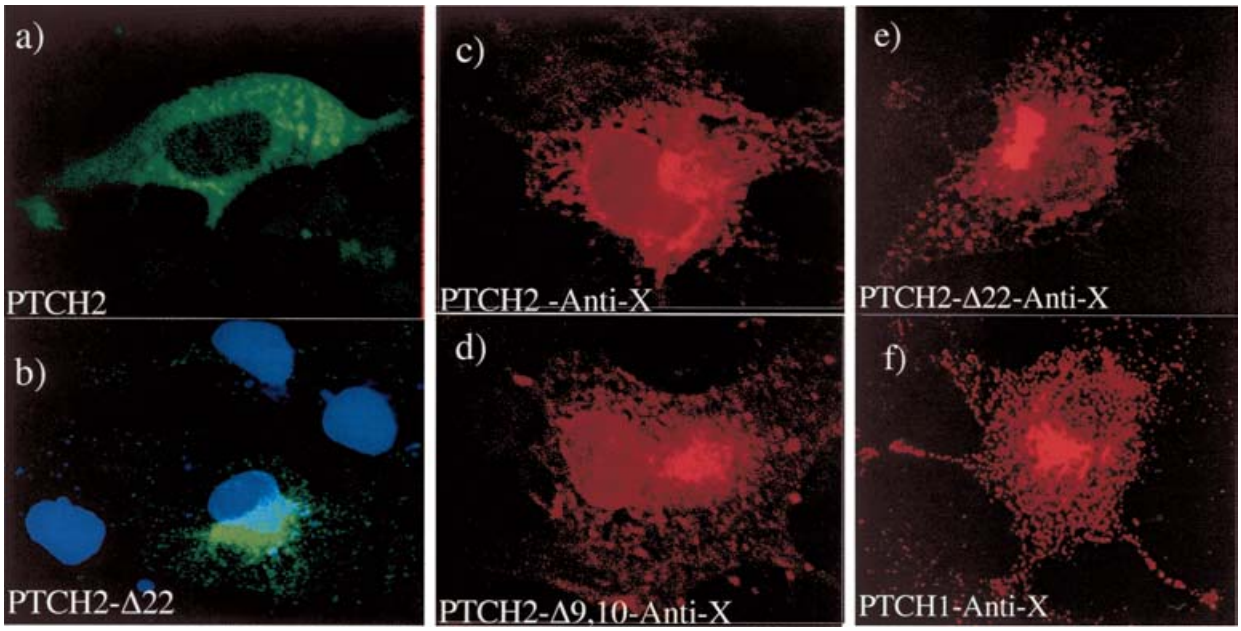

Figure 4 Subcellular localization of PTCH2 variants

COS7 cells transfected with anti-Xpress-tagged PTCH2, PTCH2-Δ9,10, PTCH2-Δ22 and PTCH1 constructs and GLI1-transfected NIH-3T3 cells were stained with antibodies to the tags or directly to PTCH2 (see the Materials and methods section). The proteins were visualized by immunofluorescence microscopy. At least 30 cells showing similar distribution were observed in each case. (**a**) NIH-3T3 cells transfected with the GLI1 expression construct and incubated with the PTCH2 antibody; (**b**) COS7 cells transfected with anti-Xpress-tagged PTCH2-Δ22 and incubated with the PTCH2 antibody. Note the presence of untransfected cells stained with the nuclear marker DRAQ^{TM}; (**c**) COS7 cells transfected with anti-Xpress-tagged PTCH2, detected with anti-Xpress antibody; (**d**) same as (**c**) but transfected with PTCH2-Δ9,10; (**e**) same as (**c**) but with PTCH2-Δ22; (**f**) same as (**c**) but with PTCH1. Patched2 (M-20) antibody with fluorescein-conjugated rabbit anti-goat IgG was used in (**a**, **b**) and anti-Xpress antibody with Rhodamine Red^{TM}-X-conjugated donkey anti-mouse IgG was used in (**c**–**f**). DRAQ^{TM} (Alexis Biochemical) nuclear staining was used in (**b**).

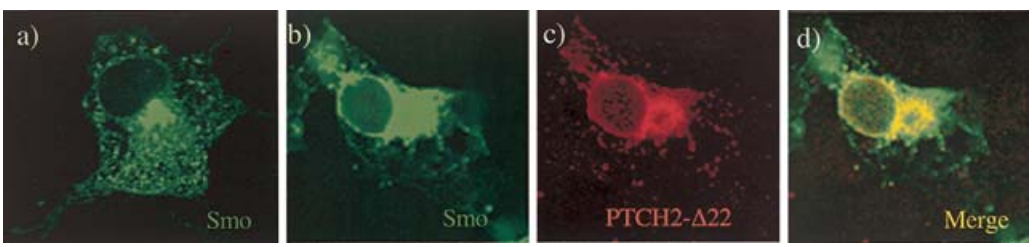

Figure 5 Altered Smo localization by the PTCH2 variants and PTCH1

COS7 cells were transfected with anti-Xpress-tagged PTCH2 variants/PTCH1 with or without HA-tagged Smo construct and stained with antibody to the respective tag. The proteins were visualized by immunofluorescence microscopy. At least 20 cells showing similar distribution were analysed in each case. (**a**) A COS7 cell transfected with Smo-HA. Single-channel confocal imaging shows dispersed cytoplasmic localization of Smo. (**b**–**d**) A COS7 cell co-transfected with PTCH2-Δ22 and Smo-HA. Dual-channel confocal imaging shows a concentrated localization of Smo together with PTCH2-Δ22. Similar results were obtained when PTCH2, PTCH2-Δ9,10 or PTCH1 were used (results not shown).

were also obtained after transfection of the epitope-tagged PTCH2 construct (results not shown). It has been proposed that *Drosophila* ptch might act indirectly to regulate smo activity, with concomitant effects on subcellular localization [28]. To test if the PTCH2 variants have the ability to alter the localization of Smo, HA-epitope-tagged Smo was transfected either alone or together with the PTCH2 isoforms as well as PTCH1. Co-transfection of Smo with either the PTCH2 variants or PTCH1 could alter the localization of Smo from being dispersed in the cytoplasm to a pattern overlapping that of the PTCH2 variants and PTCH1 (Figure 5).

Heteromeric interaction between PTCH2 variants and PTCH1

Using confocal microscopy, we determined the subcellular localization of anti-Xpress-tagged PTCH2 variants and FLAG-tagged PTCH1 in doubly transfected COS7 cells. All combinations of the PTCH2 variants when co-transfected with PTCH1 showed a similar co-localization pattern in the same cytoplasmic compartment (Figure 6a). Moreover, to investigate the possible direct interaction between the PTCH2 variants and PTCH1, HEK-293 cells were also transiently transfected with these expression constructs. A complex of the PTCH2 variants and PTCH1 was detected by co-immunoprecipitation from double-transfected cells. By calculating the amount of PTCH1 present in the lysates and in the immunoprecipitated complex, we concluded that more than 20% of input PTCH1 can be immunoprecipitated by PTCH2, suggesting that this interaction could be of physiological importance. This contrasts the $<3\%$ of input Smo or Ptch1 that can be immunoprecipitated by the other protein in this type of assay (see supplementary information in [27]), arguing against its biological relevance. Therefore these results are consistent with

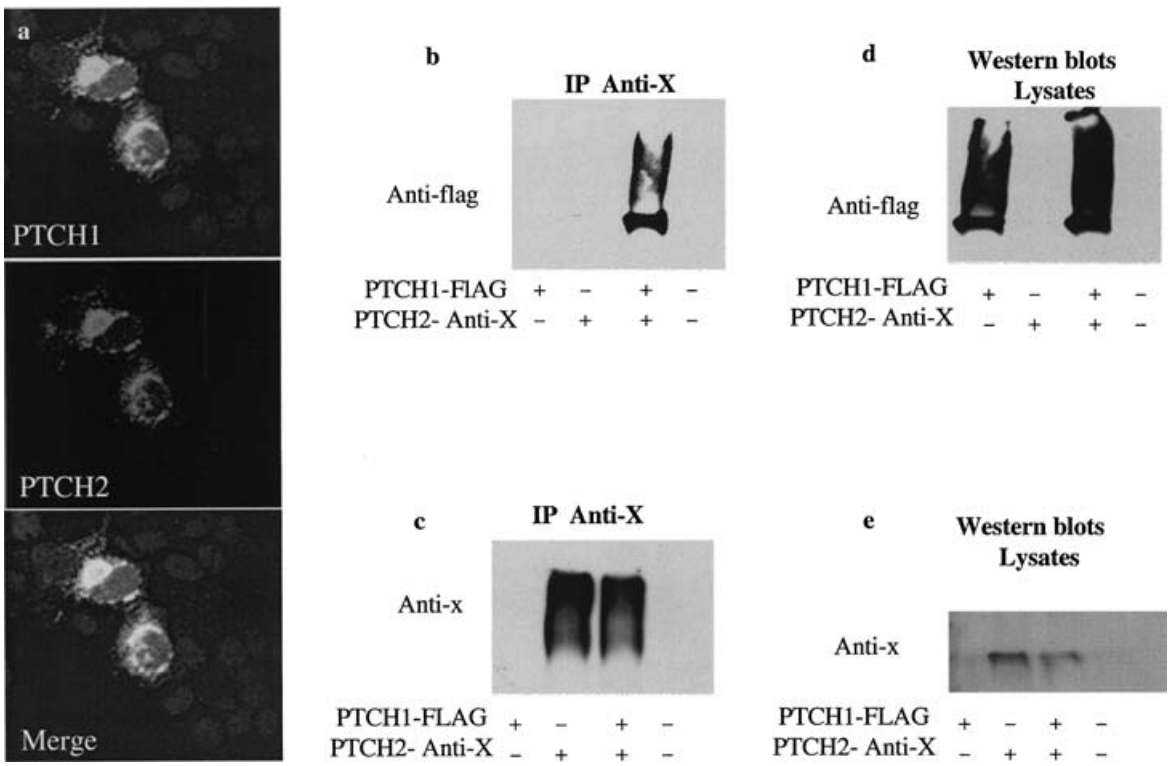

Figure 6 Heteromeric interaction between PTCH1 and the PTCH2 variants

(**a**) COS7 cells were co-transfected with anti-Xpress-tagged PTCH2 constructs and FLAG-tagged PTCH1 and stained with antibodies to anti-Xpress and the C-terminus of PTCH1 (see the Materials and methods section). Dual-channel confocal imaging shows co-localization of PTCH2 and PTCH1 in doubly transfected cells, and similar results were obtained with the other PTCH2 splice variants (results not shown). (**b**) HEK-293 cells were transfected with FLAG-tagged PTCH1 and/or anti-Xpress-tagged PTCH2 constructs. Extracts from cells transfected with either FLAG-tagged PTCH1 or with PTCH2 anti-Xpress constructs were subjected to immunoprecipitation with anti-Xpress antibodies followed by detection with FLAG antibodies in the immune complex. (**c**) Same as in (**b**) but detection was performed with anti-Xpress antibodies. (**d**) The expression of PTCH1 in cell lysates was analysed by Western blotting with FLAG antibodies. (**e**) The expression of PTCH2 in cell lysates was analysed by Western blotting with anti-Xpress antibodies. Similar results were obtained with PTCH2-Δ22 and PTCH2-Δ9,10 (results not shown).

a possible significant interaction between each of the PTCH2 variants and PTCH1 (Figures 6b–6e).

PTCH2 variants mediate internalization of Shh-N

Ptch1 functions in the receptor-mediated endocytosis of Hh proteins [29]. The ability of Ptch1 to retrieve membrane-bound Shh forms from adjacent cells indicates that removal of Shh from the extracellular milieu is an important feature of Ptch1 function, and it is probable that internalization of Shh may be linked to signal transduction. To check whether the PTCH2 variants have the same ability, C3H/10T1/2 cells were transfected with anti-Xpress-tagged PTCH2 variants followed by incubation with Shh-N, the N-terminal fragment of Shh. PTCH1 was used as control and detection was performed by immunofluorescence and confocal microscopy.

Incubation of PTCH2-transfected cells with the Shh-N peptide resulted in the appearance of internalized Shh-N within PTCH2-containing vesicles, as also seen with the PTCH1, whereas untransfected cells, present around transfected cells, showed no evidence of Shh-N uptake (Figure 7). Moreover, PTCH2-Δ22 and PTCH2-Δ9,10 were also able to internalize Shh-N, similar to the full-length PTCH2 (results not shown).

PTCH2 promoter up-regulation by SHH signalling components

As the *PTCH2* gene appears to be under the control of SHH signalling in BCCs [17] and in NIH-3T3 cells (Figure 4a), we decided to examine this regulation in more detail. First, an approx. 3.4 kb fragment of the 5′-flanking region of the *PTCH2* gene was isolated, sequenced and subcloned into the pGL3-Basic vector upstream of the firefly luciferase reporter gene (see the Materials and methods section). The presence of a GLI1-binding site (5′-TGGGTGGTC), positioned 472-463 bases upstream of the initiation ATG codon, implies a direct effect of SHH signalling in *PTCH2* activation. Then we examined whether the *PTCH2*-luc construct, after transfection into NIH-3T3 cells, was responsive to the typical activators of the pathway, SHH-N, SMO, a mutant variant of SMO (SMO-M2) that is much more potent than the wild-type [25] and GLI1. NIH-3T3 cells have been shown to be most responsive to HH induction compared with other cell lines [30]. As shown in Figure 8(a), all these activators of HH signalling could increase the level of expression of the reporter gene.

Differential effects of PTCH2 variants on SHH induction of *PTCH2*

To examine whether the PTCH2 splice variants may influence SHH-N up-regulation of the *PTCH2* promoter, co-transfection analysis was also performed. SHH-N induction was apparently inhibited by the PTCH2-Δ22 variant in a dose-dependent manner. On the other hand, for PTCH2 and PTCH2-Δ9,10, increasing the amounts of expression construct from 0.2 to 1 μg did not result in a similar pattern of inhibition (Figure 8b). Thus inclusion of exons 9 and 10 and exclusion of exon 22/inclusion of 'intron' 21 sequences are necessary for dose-dependent inhibition. Moreover, the observed PTCH1 inhibition of the SHH-N induction

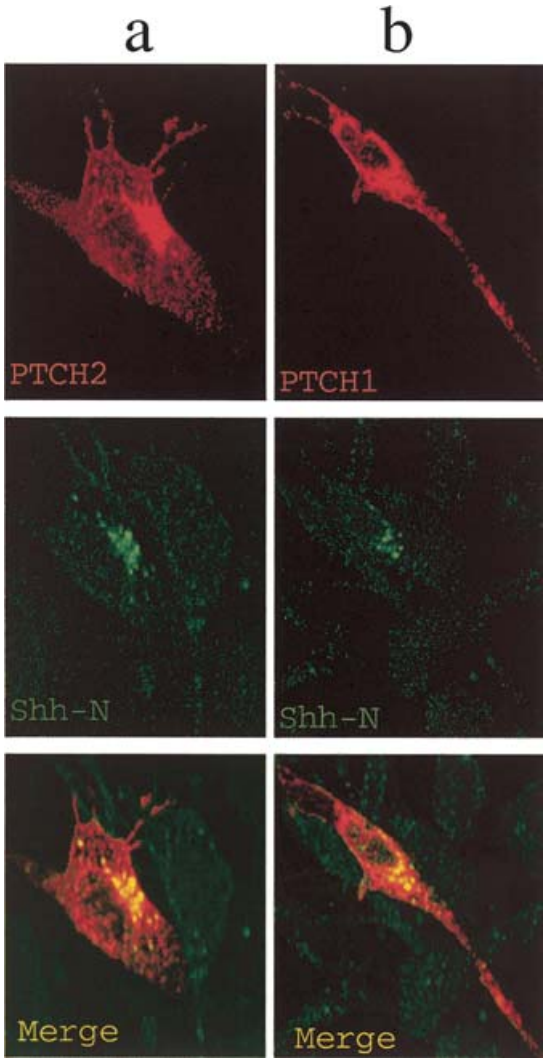

Figure 7 PTCH2 confers the ability to internalize Shh-N

C3H/10T1/2 cells expressing PTCH2 (**a**) or PTCH1 (**b**) were incubated with 1 nM Shh-N for 2 h, followed by detection with Shh-N and anti-Xpress antibodies. PTCH1 and PTCH2 were detected by single-channel confocal imaging and shown in red, whereas Shh-N is shown in green. Dual-channel imaging is indicated by yellow. Note that cells transfected with either PTCH1 or PTCH2 can internalize Shh-N, in contrast with the neighbouring non-transfected cells.

was always found to be stronger when compared with that of PTCH2-Δ22.

In contrast with these findings, SMO-M2 induction could only be inhibited by PTCH1, with the three PTCH2 splice variants apparently lacking that capacity. Increasing the amounts of the PTCH2/PTCH1 expression constructs did not substantially alter the observed pattern (Figure 8c).

Differential reconstitution of SHH transcriptional response by PTCH1/PTCH2 variants

To analyse the effects of the PTCH2 variants and PTCH1 on HH signalling in a different cellular context, we also used embryonic fibroblasts derived from *Ptch1*$^{-/-}$ mouse embryos. These cells have widespread activation of Shh target genes including Gli1 [30]. As described by Taipale et al. [30], Ptch2 activity is not detected in *Ptch1*$^{-/-}$ cells, as Shh transfection of these cells could not further increase target gene activation. As anticipated, the *PTCH2* promoter construct was found to be highly active in

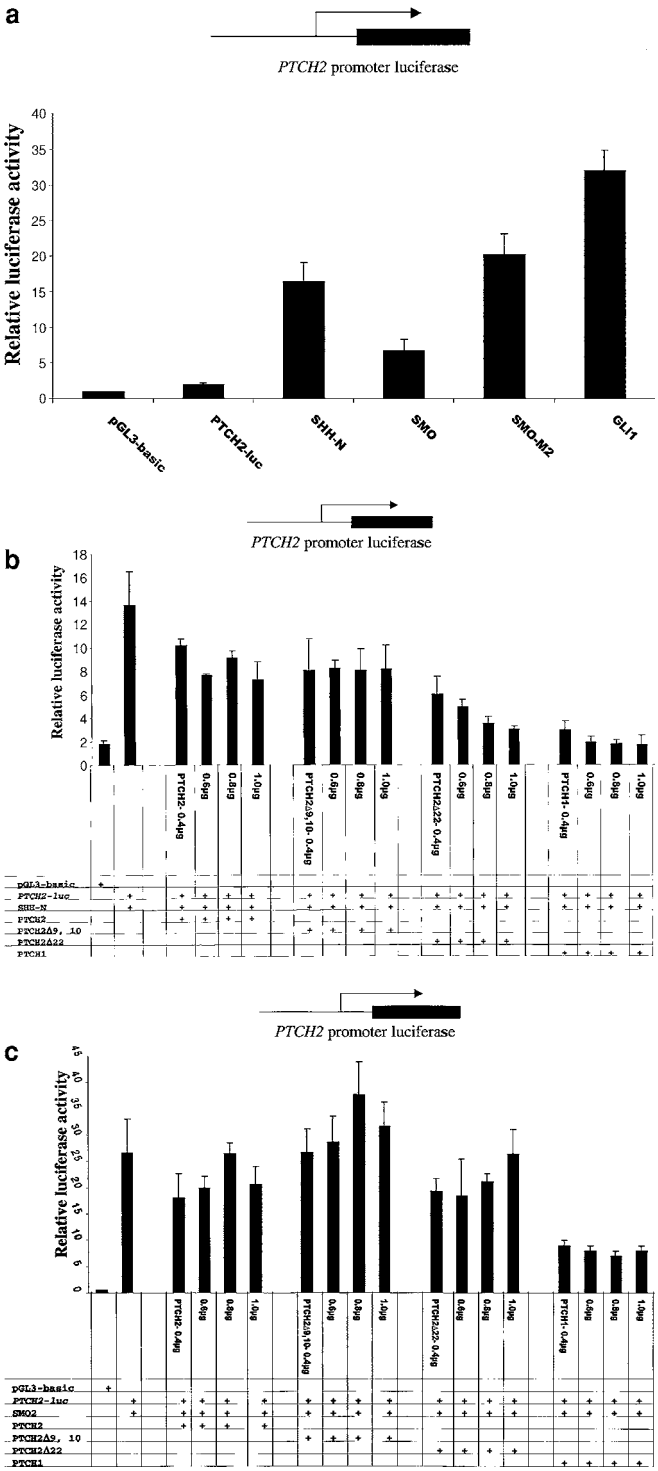

Figure 8 PTCH2 promoter is a target of HH signalling but under differential PTCH1/PTCH2 control

Confluent NIH-3T3 cells were transfected with the *PTCH2*-luc reporter construct and the indicated expression constructs. RSV-lacZ was also co-transfected as an internal control. Each data point represents an average luciferase reading of at least three separate transfection experiments normalized to the respective β-galactosidase reading. Note that by Western blotting, the expression level of the PTCH2 variants and PTCH1 constructs was found to be comparable (results not shown). (**a**) The *PTCH2* promoter can be induced by SHH-N, SMO, SMO-M2 and GLI1. (**b**) PTCH2-Δ22, but not PTCH2 or PTCH2-Δ9,10 can inhibit *PTCH2* promoter activation by SHH in a dose-dependent manner. (**c**) PTCH1, but not the PTCH2 variants, can down-regulate SMO-M2 activation of the PTCH2 promoter.

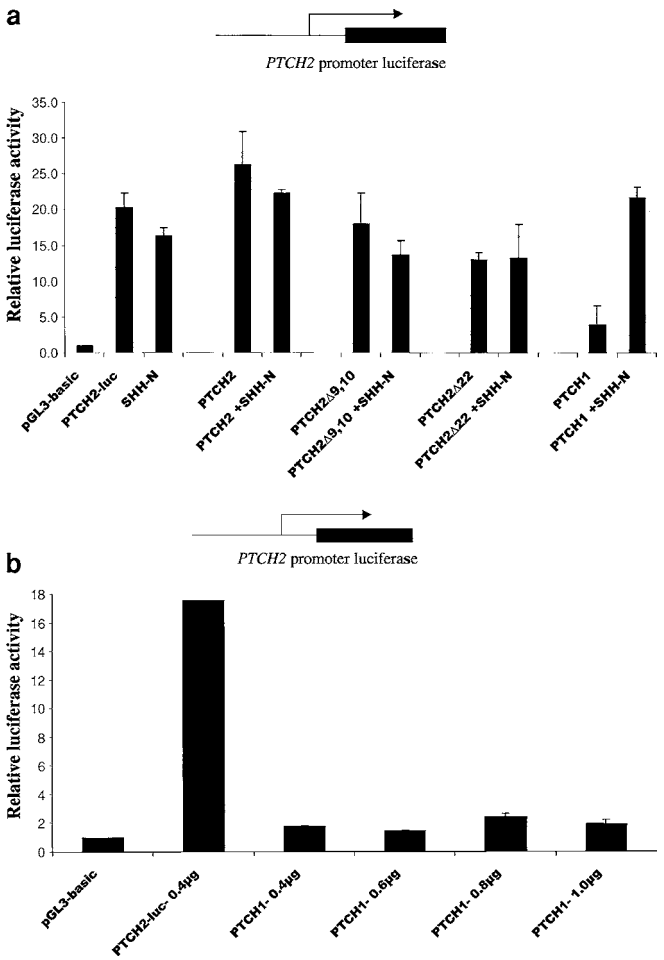

Figure 9 Analysis of the PTCH2 promoter activation in *Ptch1*$^{-/-}$ cells

(**a**) *Ptch1*$^{-/-}$ cells were transfected with the *PTCH2*-reporter, *Renilla* luciferase transfection control and expressions constructs of PTCH1/PTCH2 variants as indicated. PTCH1 could strongly inhibit the *PTCH2* promoter up-regulation. Only the PTCH2-Δ22 variant could inhibit promoter activity significantly but not to the same extent as PTCH1. This inhibition could not be relieved on co-transfection with SHH-N. (**b**) *Ptch1*$^{-/-}$ cells were transfected with the *PTCH2* reporter, *Renilla* luciferase transfection control and different amounts of PTCH1 as indicated. Note that the strong PTCH1 inhibition was already reached with 0.4 μg of expression construct.

these cells (Figure 9a). This promoter activity could be strongly inhibited by PTCH1. Only the PTCH2-Δ22 variant was capable of inhibiting the *PTCH2* promoter, but still not to the same extent as PTCH1. Additionally, the strong PTCH1 inhibition was already detected with the least amount of expression construct (Figure 9b) and a similar pattern was also observed with the PTCH2 variants (results not shown). Most interestingly, the PTCH1/PTCH2-Δ22 inhibition was relieved by SHH for PTCH1 but not for PTCH2-Δ22, implying that only PTCH1 can reconstitute a ligand-dependent transcriptional response (Figure 9a).

Differential reconstitution of DHH transcriptional response by the PTCH2 variants

Ptch2 is known to be expressed in spermatocytes, where it may mediate the function of Dhh by regulating Gli1 and Gli3 [21,31,32]. Dhh-deficient mice are sterile because of lack of mature sperm [33]. Interestingly, in testicular germ cell tumours, deletions of the chromosomal region 1p32-36 [34], the locus of the *PTCH2* gene, have been observed indicating a possible role

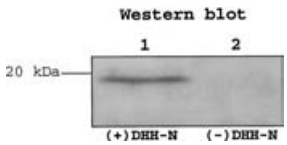

Figure 10 Detection of human DHH in HEK-293 transfected cells

Extracts of HEK-293 cells were made and subjected to Western blotting using an anti-DHH antibody. Lane 1, DHH-transfected cells; lane 2, non-transfected cells.

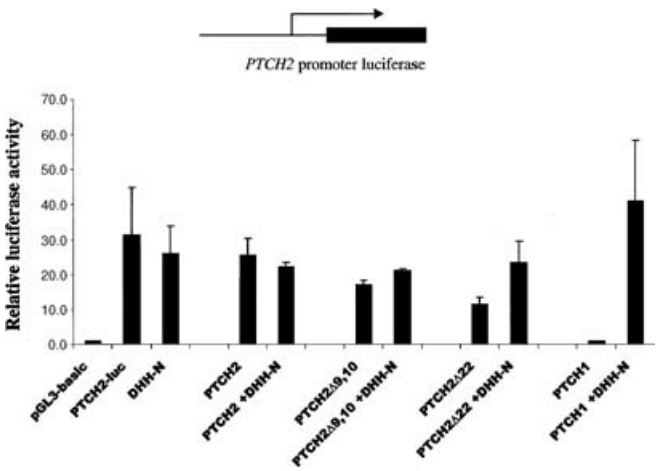

Figure 11 PTCH1 and PTCH2-Δ22 on binding to DHH can reconstitute ligand-dependent transcriptional response in *Ptch1*$^{-/-}$ cells

Ptch1$^{-/-}$ cells were transfected with the *PTCH2* reporter, *Renilla* luciferase transfection control and expressions constructs of PTCH1/PTCH2 variants as indicated. The inhibition of *PTCH2* reporter could be relieved on co-transfection of DHH-N with PTCH1 and to a lesser extent with PTCH2-Δ22 but not with PTCH2 or PTCH2-Δ9,10.

as a tumour suppressor in this setting. Our results have shown that PTCH2 is not a direct mediator of SHH signalling as is PTCH1, thus opening the possibility that PTCH2 may be an effective mediator of DHH signalling. To test this hypothesis, we generated a human DHH expression construct (see the Materials and methods section) and confirmed the synthesis of the protein by Western blotting (Figure 10). Using the Ptch1$^{-/-}$ cells, we attempted to reconstitute a transcriptional response by now employing DHH instead of SHH. PTCH2 and PTCH2-Δ9,10 were found to be inactive in this assay. However, PTCH2-Δ22-transfected cells did show a significant up-regulation in response to DHH exposure, albeit not to the same extent as PTCH1 (Figure 11).

DISCUSSION

In this study, we describe the analysis of gene products generated by the human *PTCH2* gene. In agreement with the realization that alternative splicing increases the complexity of the proteome [35], this process was found to influence *PTCH2* expression in all tissues examined. Two previously non-detected, variant PTCH2 transcripts were also identified highlighting the diverse complexity in the C-terminal region and the SSD domain, segments thought to have a role in mediating signalling. The functional significance of the splice products that either lack the last exon (PTCH2-Δ22) or exons 9 and 10 (PTCH2-Δ9,10) was examined in more detail.

Indirect immunofluorescence revealed that the localization of these splice variants is in the cytoplasm. However, direct detection of endogenous PTCH2 was only possible in NIH-3T3 cells transfected with the GLI1 expression construct, implying that signalling up-regulates PTCH2. It was shown that the PTCH2 mRNA isoforms as well as the full-length PTCH2 mRNA code for proteins that are able to change Smo localization from being dispersed in the cytoplasm to a more concentrated region near the nucleus where the PTCH2 variants are localized. Similar results were also observed with PTCH1. The mechanism of inhibition of SMO signalling by PTCH1 is not exactly known. A recent study has shown that Ptch1 inhibits Smo only when both are localized in the same cellular compartment. Shh-induced dissociation allows Smo to signal after it is sorted from the Ptch1/Shh complexes in the late endocytic pathway [36]. In an additional study, it was proposed that Ptch1 might inhibit Smo by forcing it to a subcellular compartment containing either small molecule antagonists or lacking small molecule agonists [37]. The fact that several studies in different systems have observed localization changes for SMO and PTCH1 on ligand binding shows the importance of this feature in HH signalling. However, we were not able to detect major differences among the PTCH2 variants in localization/interaction with Smo, even though alterations in the SSD domain have been implicated to influence Smo signalling [14,15]. Additionally, we could also show co-localization and heteromeric interaction between the PTCH2 variants and PTCH1 in double-transfected cells. The physiological role of this interaction is not yet known. In chick embryo [38], mouse teeth and hair bud [39,40], a close correlation between cellular sites of high Ptch2 expression and Hh signalling has been shown. Therefore it is conceivable that in some cellular contexts, PTCH1/PTCH2 interactions may be critical for an optimal biological response. Moreover, we could show that the PTCH2 variants have the same ability as PTCH1 to internalize Shh-N from the surrounding extracellular environment. PTCH1 is known to interact with caveolin, which is important in endocytosis and trafficking [41], and is also thought to act as a transporter because of its structural similarity to small molecule transporter proteins [27]. Thus PTCH1 and PTCH2 may couple both HH sequestration and the release of SMO inhibition with the late endosomal transport.

Using functional assays, we also examined whether the PTCH2 splice variants and PTCH1 could inhibit SHH induction. Results revealed dramatic differences in the extent of the inhibition observed for each of these molecules. The strongest inhibitor was found to be PTCH1. Among the PTCH2 variants, only PTCH2-Δ22 could inhibit in a dose-dependent manner, approaching at the highest dose the extent of inhibition observed with PTCH1. These findings imply that inclusion of exons 9 and 10 as well as the presence of an alternative C-terminus is essential for maximal repressor function of PTCH2. Results pointing to the same differences between the PTCH2 variants and PTCH1 were also observed using *Ptch1*$^{-/-}$ cells. In addition, the fact that the PTCH2 variants could not inhibit SMO-M2 activity, whereas PTCH1 did, albeit to a lower extent than the observed inhibition of SHH activation, further highlight the functional differences between these proteins. This SMO-M2 mutant, identified in sporadic BCCs, carries a Trp^{535} to Leu substitution in the seventh transmembrane domain, which makes the protein much more potent than the wild-type [25]. This is in agreement with our findings that PTCH1 is a stronger inhibitor of SHH when compared with SMO-M2 activation of the *PTCH2* promoter. Evidence has been presented that Ptch1 may inhibit Smo by a non-stoichiometric, catalytic mechanism making this inhibition less dependent on the dose of the Ptch1 protein [27,42], and this is consistent with our observations that decreasing the amount of PTCH1 did not change the inhibition pattern. It is probable that the generation of chimaeric constructs with interchanged PTCH1/PTCH2 domains may help delineate the PTCH1 segments responsible for repressing SMO activity.

In agreement with the observed intrinsic differences in PTCH2/PTCH1 inhibition of SHH signalling in NIH-3T3 cells, PTCH2 could not compensate for the loss of PTCH1 in BCCs [17]. This is consistent with the fact that *Ptch1*$^{-/-}$ mice die at an early embryonic stage [43,44] in spite of Ptch2 expression [45]. However, it is still conceivable and more probable that *in vivo* PTCH1 and PTCH2 are expressed at different time points and in different cell types and thus cannot compensate for each other. Such phenomena have been seen when Gli1 cDNA was knocked into the *Gli2* locus and rescued all the Shh signalling defects observed in the *Gli2*$^{-/-}$ mice [7]. This is despite the fact that *Gli2*$^{-/-}$ mice die at birth, whereas *Gli1*$^{-/-}$ mice are phenotypically normal [46].

As *Dhh*$^{-/-}$ mice have testicular abnormalities [34] and PTCH2 is expressed in testis [21], we also examined the efficiency of the PTCH2 splice variants in mediating a DHH transcriptional response. PTCH2-Δ22 had this capacity, whereas the other variants could not mediate any response. Thus PTCH2-Δ22 appears to be the biologically more significant isoform.

In summary, we have shown that the *PTCH2* promoter is under the control of the HH signalling pathway supporting a functional role of *PTCH2* in the pathway. Additionally, we demonstrated that in an appropriate cell context the PTCH2 splice variants have distinct functional properties when compared with PTCH1, with PTCH2-Δ22 consistently mediating a stronger response when compared with the other variants. The differences between PTCH2 and PTCH1 appear to reside mainly downstream of the SHH internalization step. Only the PTCH2-Δ22 variant reconstitutes DHH-dependent-signalling activation, whereas none of these variants is able to reconstitute a SHH response. However, this capacity of PTCH2-Δ22 was much weaker than that of PTCH1. Thus the expressions of splice variants of the HH receptor PTCH2 may be considered to represent a mechanism that fine tunes signalling in various cellular environments. Differences in the capacity to influence HH signalling by these two kinds of receptors can explain the inability of PTCH2 to substitute the function of mutated or deleted PTCH1 in tumours arising from disruption of this pathway. Therefore PTCH2 may have a more restricted role when compared with PTCH1, not excluding the possibility that PTCH2 could couple HH signalling to as yet unknown downstream effectors.

We thank J. Taipale (University of Helsinki, Helsinki, Finland) for providing the *Ptch1*$^{-/-}$ cells and T. Österlund and C. Finta for a critical reading of the manuscript. This study was supported by grants from the Swedish Cancer Fund and Pharmacia.

REFERENCES

1 Hahn, H., Wicking, C., Zaphiropoulos, P. G., Gailani, M. R., Shanley, S., Chidambaram, A., Vorechovsky, I., Holmberg, E., Unden, A. B., Gillies, S. et al. (1996) Mutations of the human homolog of *Drosophila* patched in the nevoid basal cell carcinoma syndrome. Cell (Cambridge, Mass.) **85**, 841–851

2 Johnson, R. L., Rothman, A. L., Xie, J., Goodrich, L. V., Bare, J. W., Bonifas, J. M., Quinn, A. G., Myers, R. M., Cox, D. R., Epstein, Jr, E. H. et al. (1996) Human homolog of patched, a candidate gene for the basal cell nevus syndrome. Science **272**, 1668–1671

3 Bellaiche, Y., The, I. and Perrimon, N. (1998) Tout-velu is a *Drosophila* homologue of the putative tumour suppressor EXT-1 and is needed for Hh diffusion. Nature (London) **394**, 85–88

4 Burke, R., Nellen, D., Bellotto, M., Hafen, E., Senti, K. A., Dickson, B. J. and Basler, K. (1999) Dispatched, a novel sterol-sensing domain protein dedicated to the release of cholesterol-modified hedgehog from signaling cells. Cell (Cambridge, Mass.) **99**, 803–815

5 Porter, J. A., Young, K. E. and Beachy, P. A. (1996) Cholesterol modification of hedgehog signaling proteins in animal development. Science **274**, 255–259
6 Pepinsky, R. B., Zeng, C., Wen, D., Rayhorn, P., Baker, D. P., Williams, K. P., Bixler, S. A., Ambrose, C. M., Garber, E. A., Miatkowski, K. et al. (1998) Identification of a palmitic acid-modified form of human Sonic hedgehog. J. Biol. Chem. **273**, 14037–14045
7 Bai, C. B. and Joyner, A. L. (2001) Gli1 can rescue the *in vivo* function of Gli2. Development **128**, 5161–5172
8 Chuang, P. T. and McMahon, A. P. (1999) Vertebrate Hedgehog signalling modulated by induction of a Hedgehog-binding protein. Nature (London) **397**, 617–621
9 Kogerman, P., Krause, D., Rahnama, F., Kogerman, L., Unden, A. B., Zaphiropoulos, P. G. and Toftgard, R. (2002) Alternative first exons of PTCH1 are differentially regulated *in vivo* and may confer different functions to the PTCH1 protein. Oncogene **21**, 6007–6016
10 Johnson, R. L., Milenkovic, L. and Scott, M. P. (2000) *In vivo* functions of the patched protein: requirement of the C terminus for target gene inactivation but not Hedgehog sequestration. Mol. Cell **6**, 467–478
11 Wang, X. Q. and Rothnagel, J. A. (2001) Post-transcriptional regulation of the gli1 oncogene by the expression of alternative 5′ untranslated regions. J. Biol. Chem. **276**, 1311–1316
12 Carstea, E. D., Morris, J. A., Coleman, K. G., Loftus, S. K., Zhang, D., Cummings, C., Gu, J., Rosenfeld, M. A., Pavan, W. J., Krizman, D. B. et al. (1997) Niemann–Pick C1 disease gene: homology to mediators of cholesterol homeostasis. Science **277**, 228–231
13 Loftus, S. K., Morris, J. A., Carstea, E. D., Gu, J. Z., Cummings, C., Brown, A., Ellison, J., Ohno, K., Rosenfeld, M. A., Tagle, D. A. et al. (1997) Murine model of Niemann–Pick C disease: mutation in a cholesterol homeostasis gene. Science **277**, 232–235
14 Martin, V., Carrillo, G., Torroja, C. and Guerrero, I. (2001) The sterol-sensing domain of Patched protein seems to control Smoothened activity through Patched vesicular trafficking. Curr. Biol. **11**, 601–607
15 Strutt, H., Thomas, C., Nakano, Y., Stark, D., Neave, B., Taylor, A. M. and Ingham, P. W. (2001) Mutations in the sterol-sensing domain of Patched suggest a role for vesicular trafficking in Smoothened regulation. Curr. Biol. **11**, 608–613
16 Johnson, R. L., Zhou, L. and Bailey, E. C. (2002) Distinct consequences of sterol sensor mutations in *Drosophila* and mouse patched homologs. Dev. Biol. **242**, 224–235
17 Zaphiropoulos, P. G., Unden, A. B., Rahnama, F., Hollingsworth, R. E. and Toftgard, R. (1999) PTCH2, a novel human patched gene, undergoing alternative splicing and up-regulated in basal cell carcinomas. Cancer Res. **59**, 787–792
18 Goodrich, L. V., Johnson, R. L., Milenkovic, L., McMahon, J. A. and Scott, M. P. (1996) Conservation of the hedgehog/patched signaling pathway from flies to mice: induction of a mouse patched gene by Hedgehog. Genes Dev. **10**, 301–312
19 Marigo, V., Scott, M. P., Johnson, R. L., Goodrich, L. V. and Tabin, C. J. (1996) Conservation in hedgehog signaling: induction of a chicken patched homolog by Sonic hedgehog in the developing limb. Development **122**, 1225–1233
20 Motoyama, J., Takabatake, T., Takeshima, K. and Hui, C. (1998) Ptch2, a second mouse Patched gene is co-expressed with Sonic hedgehog [Letter]. Nat. Genet. **18**, 104–106
21 Carpenter, D., Stone, D. M., Brush, J., Ryan, A., Armanini, M., Frantz, G., Rosenthal, A. and de Sauvage, F. J. (1998) Characterization of two patched receptors for the vertebrate hedgehog protein family. Proc. Natl. Acad. Sci. U.S.A. **95**, 13630–13634
22 Yamago, G., Takata, Y., Furuta, I., Urase, K., Momoi, T. and Huh, N. (2001) Suppression of hair follicle development inhibits induction of sonic hedgehog, patched, and patched-2 in hair germs in mice. Arch. Dermatol. Res. **293**, 435–441
23 Smyth, I., Narang, M. A., Evans, T., Heimann, C., Nakamura, Y., Chenevix-Trench, G., Pietsch, T., Wicking, C. and Wainwright, B. J. (1999) Isolation and characterization of human patched 2 (PTCH2), a putative tumour suppressor gene in basal cell carcinoma and medulloblastoma on chromosome 1p32. Hum. Mol. Genet. **8**, 291–297
24 Kogerman, P., Grimm, T., Kogerman, L., Krause, D., Unden, A. B., Sandstedt, B., Toftgard, R. and Zaphiropoulos, P. G. (1999) Mammalian suppressor-of-fused modulates nuclear-cytoplasmic shuttling of Gli-1. Nat. Cell Biol. **1**, 312–319
25 Xie, J., Murone, M., Luoh, S. M., Ryan, A., Gu, Q., Zhang, C., Bonifas, J. M., Lam, C. W., Hynes, M., Goddard, A. et al. (1998) Activating Smoothened mutations in sporadic basal-cell carcinoma. Nature (London) **391**, 90–92
26 Osborne, T. F. and Rosenfeld, J. M. (1998) Related membrane domains in proteins of sterol sensing and cell signaling provide a glimpse of treasures still buried within the dynamic realm of intracellular metabolic regulation. Curr. Opin. Lipidol. **9**, 137–140
27 Taipale, J., Cooper, M. K., Maiti, T. and Beachy, P. A. (2002) Patched acts catalytically to suppress the activity of Smoothened. Nature (London) **418**, 892–897
28 Denef, N., Neubuser, D., Perez, L. and Cohen, S. M. (2000) Hedgehog induces opposite changes in turnover and subcellular localization of patched and smoothened. Cell (Cambridge, Mass.) **102**, 521–531
29 Incardona, J. P., Lee, J. H., Robertson, C. P., Enga, K., Kapur, R. P. and Roelink, H. (2000) Receptor-mediated endocytosis of soluble and membrane-tethered Sonic hedgehog by Patched-1. Proc. Natl. Acad. Sci. U.S.A. **97**, 12044–12049
30 Taipale, J., Chen, J. K., Cooper, M. K., Wang, B., Mann, R. K., Milenkovic, L., Scott, M. P. and Beachy, P. A. (2000) Effects of oncogenic mutations in Smoothened and Patched can be reversed by cyclopamine. Nature (London) **406**, 1005–1009
31 Kroft, T. L., Patterson, J., Won Yoon, J., Doglio, L., Walterhouse, D. O., Iannaccone, P. M. and Goldberg, E. (2001) GLI1 localization in the germinal epithelial cells alternates between cytoplasm and nucleus: upregulation in transgenic mice blocks spermatogenesis in pachytene. Biol. Reprod. **65**, 1663–1671
32 Persengiev, S. P., Kondova, I. I., Millette, C. F. and Kilpatrick, D. L. (1997) Gli family members are differentially expressed during the mitotic phase of spermatogenesis. Oncogene **14**, 2259–2264
33 Bitgood, M. J., Shen, L. and McMahon, A. P. (1996) Sertoli cell signaling by Desert hedgehog regulates the male germline. Curr. Biol. **6**, 298–304
34 Summersgill, B., Goker, H., Weber-Hall, S., Huddart, R., Horwich, A. and Shipley, J. (1998) Molecular cytogenetic analysis of adult testicular germ cell tumours and identification of regions of consensus copy number change. Br. J. Cancer **77**, 305–313
35 Graveley, B. R. (2001) Alternative splicing: increasing diversity in the proteomic world. Trends Genet. **17**, 100–107
36 Incardona, J. P., Gruenberg, J. and Roelink, H. (2002) Sonic hedgehog induces the segregation of patched and smoothened in endosomes. Curr. Biol. **12**, 983–995
37 Frank-Kamenetsky, M., Zhang, X. M., Bottega, S., Guicherit, O., Wichterle, H., Dudek, H., Bumcrot, D., Wang, F. Y., Jones, S., Shulok, J. et al. (2002) Small-molecule modulators of Hedgehog signaling: identification and characterization of Smoothened agonists and antagonists. J. Biol. **1**, 10
38 Pearse, II, R. V., Vogan, K. J. and Tabin, C. J. (2001) Ptc1 and Ptc2 transcripts provide distinct readouts of Hedgehog signaling activity during chick embryogenesis. Dev. Biol. **239**, 15–29
39 Hardcastle, Z., Hui, C. C. and Sharpe, P. T. (1999) The Shh signalling pathway in early tooth development. Cell. Mol. Biol. **45**, 567–578
40 St-Jacques, B., Dassule, H. R., Karavanova, I., Botchkarev, V. A., Li, J., Danielian, P. S., McMahon, J. A., Lewis, P. M., Paus, R. and McMahon, A. P. (1998) Sonic hedgehog signaling is essential for hair development. Curr. Biol. **8**, 1058–1068
41 Karpen, H. E., Bukowski, J. T., Hughes, T., Gratton, J. P., Sessa, W. C. and Gailani, M. R. (2001) The sonic hedgehog receptor patched associates with caveolin-1 in cholesterol-rich microdomains of the plasma membrane. J. Biol. Chem. **276**, 19503–19511
42 Ingham, P. W., Nystedt, S., Nakano, Y., Brown, W., Stark, D., van den Heuvel, M. and Taylor, A. M. (2000) Patched represses the Hedgehog signalling pathway by promoting modification of the Smoothened protein. Curr. Biol. **10**, 1315–1318
43 Goodrich, L. V., Milenkovic, L., Higgins, K. M. and Scott, M. P. (1997) Altered neural cell fates and medulloblastoma in mouse patched mutants. Science **277**, 1109–1113
44 Hahn, H., Wojnowski, L., Zimmer, A. M., Hall, J., Miller, G. and Zimmer, A. (1998) Rhabdomyosarcomas and radiation hypersensitivity in a mouse model of Gorlin syndrome. Nat. Med. **4**, 619–622
45 Bailey, E. C., Milenkovic, L., Scott, M. P., Collawn, J. F. and Johnson, R. L. (2002) Several PATCHED1 missense mutations display activity in patched1-deficient fibroblasts. J. Biol. Chem. **277**, 33632–33640
46 Park, H. L., Bai, C., Platt, K. A., Matise, M. P., Beeghly, A., Hui, C. C., Nakashima, M. and Joyner, A. L. (2000) Mouse Gli1 mutants are viable but have defects in SHH signaling in combination with a Gli2 mutation. Development **127**, 1593–1605

Received 8 August 2003/14 October 2003; accepted 13 November 2003
Published as BJ Immediate Publication 13 November 2003, DOI 10.1042/BJ20031200